

Inasmuch as (u^l, c^l) is a σ correction and $\delta, \sigma \ll 1$, (u^l, c^l) may be expanded in a series in δ and evaluated at order δ^0 to obtain a valid first-order correction. The resultant equations may be integrated to provide

$$\tau^l \exp \left[\int dx/u^0 \right] + \int \exp \left[\int (u^0 + \tau^0) dx/u^{02} \right] \times d \{ u^l \exp [\pm \int \tau^0 dx/u^{02}] \} = \text{const} \quad (34)$$

$$q^l \exp \left[\int dx/u^0 \right] + \int \exp \left[\int dx/u^0 \right] d(c^l + c^0/2) = \int q^0 u^l \exp \left[\int dx/u^0 \right] dx/u^{02} + \text{const} \quad (35)$$

which, in the far field, provides an additional exponential dependence proportional to σ .

Of primary importance here is the interpretation that the effect of δ , in real flows for which $\sigma > 0$, is to allow the transported scalar to communicate velocity field details throughout the field more rapidly than the momentum equation. In particular, due to the fact that the u equation is c dependent, information on localized peculiarities in u field data is transmitted to, and affects the solution of, the (remote) u field solution via the transported scalar.

Acknowledgment

This work was carried out under contract to the Office of Basic Energy Sciences, U.S. Department of Energy.

References

- ¹Launder, B. E. and Spalding, D. B., *Mathematical Models of Turbulence*, Academic Press, N.Y., 1972.
- ²Nee, V. W. and Kovaszny, L. S. G., "Simple Phenomenological Theory of Turbulence," *The Physics of Fluids*, Vol. 12, No. 3, March 1969, pp. 473-484.
- ³Bradshaw, P., Ferriss, D. H., and Atwell, N. P., "Calculation of Boundary-Layer Development Using the Turbulent Energy Equation," *Journal of Fluid Mechanics*, Vol. 28, Pt. 3, 1967, pp. 593-616.
- ⁴Hokenson, G. J., "Transport Physics and Mathematical Characteristics," *AIAA Journal*, Vol. 17, July 1979, pp. 781-783.

Noniterative Cross-Flow Integration for the Pressure-Split Analysis of Subsonic Mixing-Layer Problems

S. M. Dash* and N. Sinha†

Science Applications, Inc., Princeton, New Jersey

Introduction

THE spatial marching analysis of subsonic, quasiparabolic mixing-layer problems is commonly performed using the numerical artifice of pressure splitting.¹⁻³ In the pressure-split approach, the governing parabolized Navier-Stokes (PNS) equations are spatially integrated with the streamwise pressure gradient "imposed," and the cross-flow pressure variation determined a posteriori, at each integration step, from the coupled solution of the continuity and cross-flow

momentum equations. Thus, the stepwise integration is comprised of 1) a standard parabolic integration yielding the streamwise component of velocity and pertinent scalar (total enthalpy, species) and turbulence model variables; and 2) an elliptic-like cross-flow integration yielding the cross-flow velocity components and pressure variation. Subsequent upgrades to the solution based on a global pressure iteration can be performed in regions with strong pressure gradients.

While the parabolic streamwise integration procedures are comparable in most models, the details of the local and global pressure-splitting procedures are problem dependent, and the cross-flow solution techniques vary widely. The continuity and cross-flow momentum equations are strongly coupled through the pressure, density, and cross-flow velocity derivatives, and are solved in an iterative manner. In the popular approach of Patankar and Spalding,¹ a pressure-correction equation arrived at from the continuity equation (with cross-flow momentum constraints) is used to determine the cross-flow pressure variation, while the cross-flow velocities are determined from the momentum equations. In contrast, the two-dimensional iterative procedure of Bradshaw and coworkers^{3,4} employs the continuity equation to determine the cross-flow velocity and the normal momentum equation to determine the pressure variation.

In utilizing pressure-split methodology for the two-dimensional analysis of curved wall jets⁵ and subsonic regions of underexpanded free jets^{6,7} (i.e., behind Mach disks and between the jet mixing-layer sonic line and jet outer edge), Dash and coworkers initially utilized the cross-flow procedure of Bradshaw and coworkers. In assessing this procedure, it was found that the iterative sweeps required between the continuity and cross-flow momentum equation solutions could be eliminated by combining these equations into a unified equation for the cross-flow velocity. This provides a considerable savings in overall computer time and eliminates possible convergence problems occurring in iterative approaches. This Note describes this new noniterative procedure and its application to a simple two-dimensional curved wall jet problem.

It should be noted that this new technique extends the efficiency of single-sweep pressure-splitting methodology to a level whereby PNS mixing solutions can be obtained in slightly more time than that required for standard parabolic mixing solutions. The results provided using this rapid procedure are identical to those obtained using previous iterative, pressure-split methodology as ascertained by numerical experiments. Hence, the favorable comparisons with data obtained using the curved wall jet and free jet models of Refs. 5-7 remain unchanged, and, the results of Bradshaw and coworkers^{3,4} would be reproduced using this approach if all other aspects of the computational procedure and turbulence modeling were duplicated.

Cross-Flow Analysis

The overall mixing-layer analysis is performed in mapped, surface-oriented curvilinear coordinates using the upwind, implicit formulation described in Ref. 5. With the rectangular mapping

$$\xi = s \quad \eta = n/\delta(s) \quad (1)$$

(where s is the streamwise direction, n is normal to it, and $\delta(s)$ is the width of the mixing zone) the parabolized, planar normal momentum equation can be written⁵:

$$\rho U \frac{\partial V}{\partial \xi} + \rho \tilde{V} \frac{\partial V}{\partial \eta} + b h \frac{\partial P}{\partial \eta} + K \rho U^2 = g_v \quad (2)$$

where $\tilde{V} = b h V - a U$; K is the curvature, h a curvature parameter ($= 1 - nK$); a and b mapping parameters; and g_v contains the laminar and turbulent stress terms.⁵

Received Oct. 11, 1983; revision received Feb. 7, 1984. Copyright © American Institute of Aeronautics and Astronautics, Inc., 1984. All rights reserved.

*Technical Director, Propulsion Gas Dynamics Division. Member AIAA.

†Research Scientist, Propulsion Gas Dynamics Division. Member AIAA.

The mapped continuity equation takes the form

$$\frac{\partial}{\partial \xi} \left(\frac{\rho U}{b} \right) + \frac{\partial}{\partial \eta} \left(h \rho V - \frac{a}{b} \rho U \right) = 0 \quad (3)$$

The density derivatives in Eq. (3) can be related to pressure, velocity, and total enthalpy derivatives via differentiating the state relation yielding

$$d\rho = [\gamma dP + (\gamma - 1)\rho(UdU + VdV - dH)]/C^2 \quad (4)$$

where $C^2 = \gamma P/\rho$. Noting that

$$\frac{\partial P}{\partial \xi} = \frac{\partial P^*}{\partial s} + a \frac{\partial P}{\partial \eta}$$

where $\partial P^*/\partial s$ is the imposed streamwise pressure gradient, combining Eqs. (3) and (4) yields the modified continuity relation

$$\begin{aligned} \gamma \left(a + \frac{\tilde{V}}{U} \right) \frac{\partial P}{\partial \eta} + (\gamma - 1) \rho V \frac{\partial V}{\partial \xi} \\ + \left[\frac{\rho b h C^2}{U} + (\gamma - 1) \frac{\rho V \tilde{V}}{U} \right] \frac{\partial V}{\partial \eta} = g_p \end{aligned} \quad (5)$$

where the source term g_p (whose terms are known from the streamwise parabolic integration performed apriori) is given by

$$\begin{aligned} g_p = \rho b C^2 \frac{\partial}{\partial \eta} \left(\frac{a}{b} \right) + K \rho C^2 \frac{V}{U} - \left[\frac{\rho C^2}{U} + (\gamma - 1) \rho U \right] \frac{\partial U}{\partial \xi} \\ + \left[\frac{\rho a C^2}{U} - (\gamma - 1) \rho \tilde{V} \right] \frac{\partial U}{\partial \eta} + (\gamma - 1) \rho \left[\frac{\partial H}{\partial \xi} + \frac{\tilde{V}}{U} \frac{\partial H}{\partial \eta} \right] \\ - \gamma \frac{\partial P^*}{\partial s} + \frac{\rho C^2}{b} \frac{\partial b}{\partial \xi} \end{aligned}$$

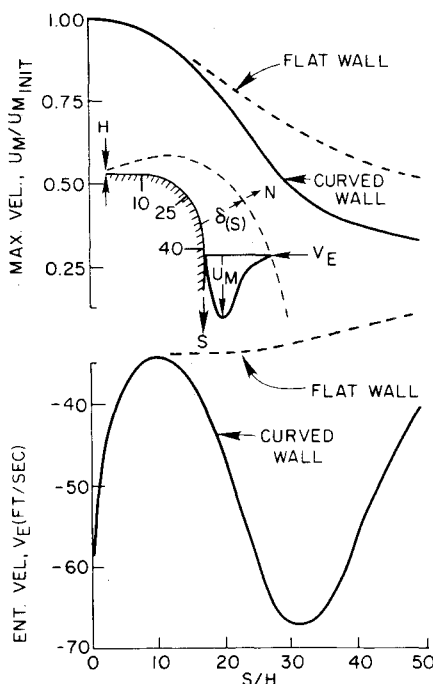


Fig. 1 Streamwise variations of maximum jet velocity and entrainment velocity for wall jet on flat and curved surfaces.

Equations (2) and (5) uniquely define the cross-flow velocity and pressure variation and are readily combined into a single equation for V by eliminating the $\partial P/\partial \eta$ term. This yields an equation of the form

$$A_1 \frac{\partial V}{\partial \xi} + A_2 \frac{\partial V}{\partial \eta} = G(V) \quad (6)$$

which can be solved without requiring any assumptions concerning the cross-flow pressure variation. Equation (6) has been integrated explicitly (treating the stress terms as forcing functions) via a two point upward integration from the wall or axis of symmetry. Utilizing this approach within the confines of a fully implicit procedure for the solution of the streamwise parabolic equations⁵ has presented no stability problems. The cross-flow pressure variation is subsequently determined via a downward trapezoidal integration of Eq. (2) utilizing the predicted V distribution and initiated with the prescribed outer-edge pressure.

Curved Wall Jet Calculation

The calculation described was performed for an initially sonic wall jet exhausting into still air, undergoing a 90 deg turn over the convex surface depicted in Fig. 1. The surface curvature K is zero for the first 10 slot heights, varies quadratically from $10 < S/H < 40$ with a peak value at $S/H = 25$ corresponding to a radius of curvature of 12.5 slot heights, and is zero for $S/H > 40$. The predicted jet boundary growth (Fig. 1) exhibits that the jet width at the position of maximum curvature is comparable to the surface radius of curvature. The predicted decay of maximum streamwise velocity and the variation of the entrainment (outer, normal influx) velocity are compared with the corresponding values for a flat surface in Fig. 1. The curvature significantly enhances the rate of mixing and, hence, the streamwise velocity decay and inward entrainment velocities. Note the rapid departure of the curved and flat wall entrainment velocity distributions beyond $S/H = 10$; the location of peak entrainment velocity at $S/H \sim 30$, downstream of the peak curvature position; and the rapid approach of the curved wall value to the flat wall value beyond $S/H = 40$, where the curvature terminates. The calculations were performed using the curvature-corrected⁸ two-layer turbulence model (inner damped Van Driest, outer $k\epsilon$) described in Ref. 5.

The predicted pressure variations along the curved surface utilizing the viscous and inviscid forms of the normal momentum equation are exhibited in Fig. 2. The

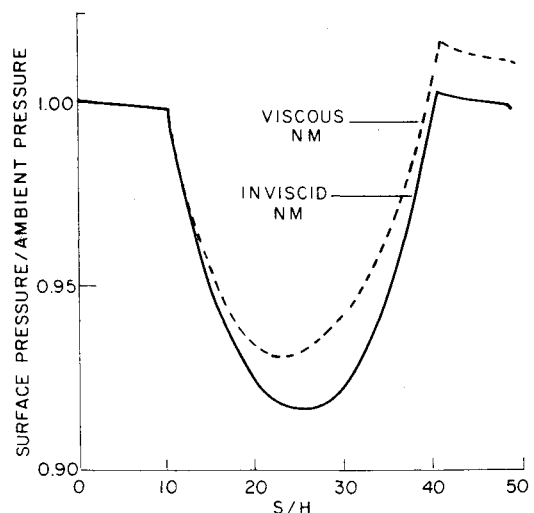


Fig. 2 Streamwise variation of surface pressure using viscous and inviscid forms of normal momentum equation.

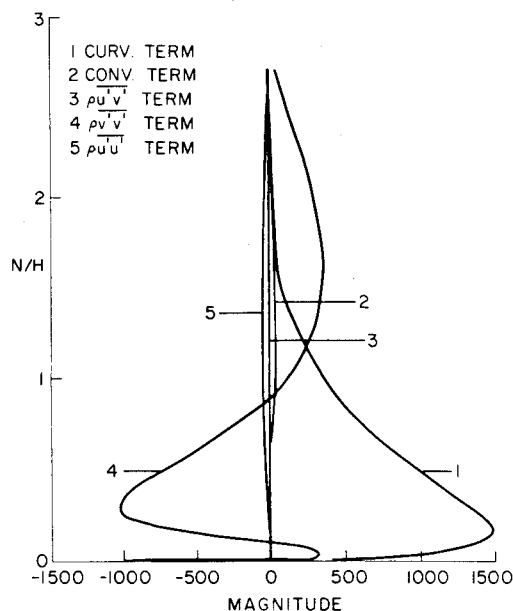


Fig. 3 Contribution of curvature, convective, and turbulent stress terms to normal pressure variation across wall jet at $S/H = 15$.

viscous/turbulence terms tend to reduce the deviation of the wall pressure from the external stream value. Note that the inviscid pressure is minimum at the peak curvature position of $S/H = 25$ while the viscous value is minimum somewhat upstream. The contribution of the various terms in the normal momentum equation to the pressure variation across the curved wall jet is exhibited in Fig. 3 at the position $S/H = 15$. The dominant term, as expected, is the surface curvature term ($K\rho U^2$). Using standard Boussinesq modeling for the turbulent stress terms, viz.

$$-\rho \overline{u'_i u'_j} = -\frac{2}{3} \rho k \delta_{ij} + \mu_t \left[\left(\frac{\partial U_i}{\partial X_j} + \frac{\partial U_j}{\partial X_i} \right) - \frac{2}{3} \text{div } \vec{V} \right] \quad (7)$$

(see Ref. 5 for the specific parabolized terms retained in curvilinear s, n coordinates) the dominant viscous contribution comes from the $\rho v'v'$ stress term. This term acts counter to the surface curvature term over a significant portion of the wall jet. Comparable profiles at other stations and further details of this calculation are available in Ref. 9.

Concluding Remarks

The noniterative cross-flow procedure described has proven to be an efficient and reliable improvement to the two-dimensional iterative cross-flow procedure of Bradshaw and coworkers.^{3,4} Comparable results with the Bradshaw method typically required two to three iterative sweeps at each station. Parabolic mixing-layer codes can be extended readily to incorporate this cross-flow procedure, and their "direct coupling" with an external potential flow solution^{3,4} provides a simple extension of boundary-layer interactive concepts to situations with large normal pressure variations. The authors have formulated a "semi-iterative" extension of this approach to three-dimensional mixing-layer problems via analogous manipulations of the continuity and cross-flow momentum equations which will be described in a future article.¹⁰

Acknowledgments

This work was partially supported by David Taylor Naval Ship Research and Development Center under Contract N00167-83-C-0082 and by NASA Langley Research Center under Contract NAS1-16535.

References

- ¹Patankar, S. V. and Spalding, D. B., "A Calculation Procedure for Heat, Mass, and Momentum Transfer in Three-Dimensional Parabolic Flows," *International Journal of Heat and Mass Transfer*, Vol. 15, Oct. 1972, pp. 1787-1806.
- ²Briley, W. R., "Numerical Method for Predicting Three-Dimensional Steady Viscous Flow in Ducts," *Journal of Computational Physics*, Vol. 14, 1974, pp. 8-28.
- ³Mahgoub, H.E.H. and Bradshaw, P., "Calculation of Turbulent-Inviscid Flow Interactions with Large Normal Pressure Gradients," *AIAA Journal*, Vol. 17, Oct. 1979, pp. 1025-1029.
- ⁴Chen, Z. B. and Bradshaw, P., "Calculation of Viscous Transonic Flow Over Airfoils," *AIAA Journal*, Vol. 22, Feb. 1984, pp. 201-205.
- ⁵Dash, S. M., Beddini, R. A., Wolf, D. E., and Sinha, N., "Viscous/Inviscid Analysis of Curved Sub- or Supersonic Wall Jets," *AIAA Journal*, Vol. 23, Jan. 1985, pp. 12-13; also, AIAA Paper 83-1679, July 1983.
- ⁶Dash, S. M. and Wolf, D. E., "Interactive Phenomena in Supersonic Jet Mixing Problems, Part I: Phenomenology and Numerical Modeling Techniques," *AIAA Journal*, Vol. 22, July 1984, pp. 905-913.
- ⁷Dash, S. M. and Wolf, D. E., "Fully-Coupled Analysis of Jet Mixing Problems, Part I: Shock-Capturing Model, SCIPVIS," NASA CR 3761, Jan. 1984.
- ⁸Lauder, B. E., Priddin, C. H., and Sharma, B. I., "The Calculation of Turbulent Boundary Layers on Spinning and Curved Surfaces," *ASME Journal of Fluids Engineering*, Vol. 99, March 1977, pp. 231-239.
- ⁹Dash, S. M. and Sinha, N., "Pressure-Split Extensions of SPLITWJET Model for Wall Jet/Potential Flow Coupling," Science Applications, Inc., Princeton, N.J., SAI/PR TR-17, Feb. 1984.
- ¹⁰Dash, S. M., Wolf, D. E., and Sinha, N., "Parabolized Navier-Stokes Analysis of Three-Dimensional Jet Mixing Problems," AIAA Paper 84-1525, June 1984.

Emmons Spot Forcing for Turbulent Drag Reduction

Wesley L. Goodman*

NASA Langley Research Center, Hampton, Virginia

Nomenclature

C_F/C_{FH}	= skin-friction coefficient normalized by skin-friction coefficient at maximum frequency
f	= frequency, Hz
Re_θ	= Reynolds number based on momentum thickness
St	= Strouhal number, $= f\delta/U_\infty$
U_∞	= freestream velocity
V'_w	= acoustic perturbation velocity
Z	= transverse coordinate
δ	= boundary-layer thickness
θ	= boundary-layer momentum thickness

Introduction

THE viscous or skin-friction drag associated with a turbulent boundary layer accounts for approximately 50% of the drag on conventional takeoff and landing (CTOL) aircraft and surface ships and nearly all of the pumping power in long-distance pipelines. Reduction of this viscous drag would allow longer range, reduced fuel volume/cost, and/or

Received Oct. 4, 1983. Revision received Jan. 23, 1984. This paper is declared a work of the U.S. Government and therefore in the public domain.

*Aerospace Engineer, Turbulent Drag Reduction Group, Viscous Flow Branch, High-Speed Aerodynamics Division.